



UPPSALA  
UNIVERSITET

UPTEC Q 20 008

Examensarbete 30 hp

September 2021

# Characterization of surface defects caused by ultrasonic cleaning of aluminium

---

Emanuel Eriksson

Civilingenjörsprogrammet i teknisk fysik med  
materialvetenskap



UPPSALA  
UNIVERSITET

## Characterization of surface defects caused by ultrasonic cleaning of aluminium

---

Emanuel Eriksson

### **Abstract**

This master thesis studies the behaviour of two aluminium alloys in ultrasonic cleaning at two different intensities, as well as the effect of a cleaning solution, Formula 815 GD-NF on the same surface have been studied with respect to surface roughness and material composition. Methods like Light Optical Microscopy (LOM), Scanning Electron Microscopy (SEM), Energy Dispersive Spectroscopy (EDS) and 3D topography using white light interferometry (VSI) was used to study the surface and material composition.

It was found that both the ultrasonic cleaning, as well as the solution itself both increase surface roughness of the samples. When crossing a threshold in ultrasonic intensity micro jet cavitation dislodge precipitates, or areas weakened by precipitate to form a large pit. And the following heat from the jet causes the surface to oxidise, becoming more brittle, and be broken up by other cavitation phenomena to cause rapid acceleration of surface roughness in an area originating from the pit.

**Teknisk-naturvetenskapliga fakulteten**

**Uppsala universitet, Utgivningsort Uppsala/Visby**

Handledare: Christian Ulrich Ämnesgranskare: Staffan Jacobsson

Examinator: Åsa Kassman Rudolphi

## Karakterisering av ytdefekter från ultraljudsrengöring av aluminium

*Författare:*

EMANUEL ERIKSSON

Få saker är så väsentliga inom luftfartsindustrin som pålitlighet, precision, och kvalitet. Allting måste fungera, och svängrummet för fel är obefintligt. Därför väljer företag som t.ex. Saab att producera vissa av sina komponenter själva.

Att producera detaljerna är en mycket komplicerad process där delar fräses ut ur stora gjutna block, och blir då täckta i allt ifrån skärvätska, rester ifrån skärverktygen, och också metallflisor som lägger sig på ytan. Ingen av dessa föroreningar får finnas kvar när detaljerna går vidare i produktionen, då de kan göra att delar avviker från tolleranser, öka risken för tre-kroppars abrasion, samt utgöra angreppspunkter för korrosion. Ett sätt att öka tvätteffekten är att använda ultraljudstvätt.

Ultraljudstvätt fungerar genom att sänka ner materialet i ett kar fyllt med en rengöringsvätska, och sen slå på stora transduktorer under vattnet som fyller karet med högfrekventa ultraljudsvågor. Dessa resonerar med små gasbubblor i vätskan och gör att trycket sänks i bubblorna. Ett minskat tryck gör att kokpunkten sänks, och gasen börjar expandera. När sen bubblorna växt, och trycket från den omgivande vätskan blir för högt, så kollapsar bubblorna med en explosionsartad kraft, och det är just den kraften som gör att ultraljudsrengöring är så effektiv som den är. För den kraften gör att både en chockvåg slår ut från bubblan, som då skakar sönder smutsen på ytan, och gör att rengöringsmedlet har större yta att verka på. Kraften höjer också temperaturen i vätskan, vilket gör att kemin fungerar snabbare. Och slutligen så gör alla tusentals kollapser att vattnet blir relativt turbulent, vilket hjälper till med att föra bort den bortslagna smutsen från ytan, och bidrar till att ny rengöringsvätska alltid kan vara i kontakt med smutsen. Allt detta, även på områden där ingen skurborste har en chans att komma åt.

Det är också just den här kraften som gör att ultraljudsrengöring också kan leda till erosion. Om effekten är för hög, kan det leda till att det inte bara är smutsen som slås sönder och börjar forslas bort från ytan, utan även att materialet börjar

eroderas.

I och med att man önskar byta från det rengöringsmedel man använder idag, till ett mer miljövänligt alternativ, så kommer man att behöva justera effekten på ultraljudstvätten. Och det är effekten av en ökad intensitet, och ett nytt rengöringsmedel på två av de aluminiumlegeringar man använder som detta arbete har försökt identifiera.

Genom att se hur ytojämnheten utvecklades med tiden för provbitar som legat i tvättvätskan utan någon ultraljudstvätt kunde den utvärderas separat. Samma kontroll av ytojämnheten gjordes även för provbitar som gått olika länge i ett ultraljudsrengörings-program på 50 % intensitet. Detta för att sakta ner erosionsförloppet och bättre hinna se hur ytojämnheten förändrades. Till slut tvättades även provbitar vid 100 % intensitet, för att utvärdera de defekter som uppstår då nästan omedelbart.

Med hjälp av ljusinterferometri, ljusoptiskmikroskopi samt elektronmikroskopi har ytojämnheten kunnat mätas, och även bilder med hög upplösning tas för att utvärdera ytan och de gropar och "moln" som bildats på ytan av provbitarna vid den högsta intensiteten. Och tillslut kunde dessa analyseras med EDS (Energy-dispersive X-ray spectroscopy) för att avgöra om man såg en skillnad i legeringens sammansättning, och om det kunnat bidra till erosionen.

Resultaten visar att ytan blivit grövre, orsakat både av rengöringsvätskan i sig och av ultraljudstvätten. Vid den högsta intensiteten bildades djupa gropar på ytan, med stora utskjutande moln formade som kometsvansar runt om mittdelen av provbitarna som testats. Dessa visade sig bero på att legeringsämnen separerat, och sedan slagits loss från ytan av ultraljudsfenomenen, och genom värmen och kraften hade ytan deformerats och blivit långt mycket ojämnare.

**Examensarbete 30 hp på civilingenjörsprogrammet  
Teknisk fysik med materialvetenskap  
Uppsala universitet, januari 2022**

## ACKNOWLEDGEMENTS

I am deeply appreciative of all the support, and great connection that I have received from the team at Saab. Leaving the safe world of studies that I have been comfortable in for so long, for something new felt both scary, and intimidating. But the response and support you've given me have made this step one of the most enjoyable, safe, and rewarding steps of my "study-career" so far. Christian, the support I've felt you've given me has been unmatched. To feel that you've prioritized and made an effort to help me at every step is one of the main reasons to why I have felt as safe as I have to be able to do what I have done. Thanks to Johanna for all the support and guidance I could ever need in the workshop and regards to samples. Thanks to Peter for more than one idea, and for always lightening the mood.

Furthermore, I'd like to thank Victoria for the help in the microstructure laboratory, both with tips, support, and a healthy dose of patience. Speaking of patience, this acknowledgement would not feel complete without mentioning Staffan and Åsa. Staffan, you've given me a new way of looking at reports, and my process, and for this, I do not believe this report could've been nearly as good as I feel it has finally become. Thank you Åsa for patience and help, even though I am fully aware Head of department might take a substantial amount of time, and me complicating things with contracts and NDA:s didn't exactly make it a smooth and linear experience...

To my dear Katrin, I would not have made it without you and your support. I am truly grateful.

Last but definitely not least, big thanks to Johan, Ludvig and Erik that helped me stay focused and have an, as you wanted me to describe it: " $A_{WS}^E OM^E$ " time during the last weeks of writing the report.

THIS PAGE HAS INTENTIONALLY BEEN LEFT BLANK.

# Contents

	Page
Abstract	I
Populärvetenskaplig sammanfattning	III
Acknowledgements	V
List of Figures	VIII
List of Tables	VIII
<b>1 Introduction</b>	<b>1</b>
1.1 Background . . . . .	1
1.2 Aim and Objectives . . . . .	1
1.3 Limitations . . . . .	2
<b>2 Theory</b>	<b>3</b>
2.1 Ultrasonic Cavitation . . . . .	3
2.1.1 Spherical bubble collapse . . . . .	4
2.1.2 Non-spherical bubble collapse . . . . .	4
2.1.3 Geometric influence . . . . .	4
2.2 Ultrasonic cleaning . . . . .	5
2.2.1 Cavitation erosion . . . . .	5
<b>3 Experimental</b>	<b>6</b>
3.1 Materials . . . . .	6
3.2 The effect of the cleaning solution on the surface . . . . .	7
3.3 Samples ultrasonically cleaned at different intensities . . . . .	7
3.4 Surface roughness evaluation and presentation . . . . .	7
3.5 Pre- and post characterization of the surfaces . . . . .	7
<b>4 Results</b>	<b>8</b>
4.1 Surface appearance and elemental analysis . . . . .	8
4.1.1 General observations on the similarities between 2050 & 7050	8
4.1.2 Surface appearance of the raw samples . . . . .	8
4.1.3 Samples ultrasonically cleaned at 50 % intensity . . . . .	9
4.1.4 Samples ultrasonically cleaned at 100 % intensity . . . . .	9
4.1.5 Influence of cleaning process duration on general surface rough-	12
ness . . . . .	
<b>5 Discussion</b>	<b>14</b>
5.1 Surface overview and imaging . . . . .	14
5.1.1 Effects of the cleaning liquid and ultrasonic washing on ma-	14
terial surface . . . . .	
5.1.2 Pit and cloud development and characterization . . . . .	15

<b>6</b>	<b>Conclusions</b>	<b>16</b>
<b>7</b>	<b>Further research</b>	<b>18</b>
	<b>References</b>	<b>19</b>

## List of Figures

	<b>Page</b>
FIGURE 1 - Graphical representation of the growth and collapse of acoustic cavitation bubbles .....	3
FIGURE 2 - Illustration of the spherical bubble collapse versus the non-spherical collapse and the resulting loading on a surface .....	4
FIGURE 3 - Images of the sample production process. ....	6
FIGURE 4 - BSE image of 7050 surface on a raw sample, showing lighter particles that show up as Cu and Fe rich areas. ....	8
FIGURE 5 - Representative of the average surface of a raw 7050-sample. SEM-image. The separated elements have been identified using the EDS maps in the bottom row (Al, Mg, Cu; 20 kV).....	9
FIGURE 6 - Average of five measurements. Values with standard deviation of $R_a$ values against time. The blue graph shows results from samples cleaned with an ultrasonic cleaner turned on at 50% intensity. The red line shows samples left in the cleaning solution with the ultrasonic cleaner turned off.	10
FIGURE 7 - Typical LOM image of representative 7050 surface.....	10
FIGURE 8 - LOM image of a sample, pits and clouds marked with red rings.	11
FIGURE 9 - Representative LOM image of area with pits and clouds, bigger ones marked in image.....	11
FIGURE 13 - Pit tilted at 60° for better contrast at two magnifications.	11
FIGURE 10 - Image of typical pit. Cloud direction is downward in the image. SEM secondary electron image.....	12
FIGURE 11 - Magnified image of a cloud. SEM secondary electron image.	12
FIGURE 12 - SEM image where areas for further element identification are marked. The separated elements have been identified using the EDS maps in the bottom row (Al, Si, Ca, O, C; 20 kV).....	13

## List of Tables

	<b>Page</b>
TABLE 1 - Chemical composition of the 2050 Al-alloy given in % volume.	6



TABLE 2 - Chemical composition of the 7050 Al-alloy.....	6
TABLE 3 - Quantitative EDS analysis of 2050 sample after 12 minutes of ultrasonic cleaning at 100 % intensity. ....	13
TABLE 4 - Quantitative EDS analysis of 7050 sample after 12 minutes of ultrasonic cleaning at 100 % intensity. ....	13

# 1 Introduction

This master thesis project was performed at Saab Aeronautics in Tannefors, Sweden, for 20 weeks. The aim was to determine the chemical make-up and origin of the surface defects generated in aluminium when cleaned for extended periods of time in ultrasonic baths.

## 1.1 Background

In the highly custom and regulated field of aeronautics, most parts created are custom, highly complex, and made specifically for each use-case. This low volume production is the reason why most parts are created in house, by a subtractive manufacturing operation. This method enables complete customization, as well as conserving manufacturing secrets. Machining is, however, a dirty process in comparison to similar manufacturing processes. It requires well tailored cleaning processes to ensure the perfect finish, and guaranteed result, required in the aviation industry.

This can be achieved with physical or chemical processes or by a combinations of the two. Ultrasonic cleaning in combination with a detergent is an example of one of these combined processes, and is a process used for surfaces where a completely clean surface is uncompromisable. This technique combines the physical cleaning effect of the ultrasonic cleaner with the chemical process from a detergent to achieve a deep and thoroughly clean surface without necessarily using environmentally hazardous chemicals. One of the downsides of a combined process like this is the risk of cavitation erosion. The cavitation erosion phenomena consist of the formation, growth, and collapse of microscopic bubbles induced in a liquid by big fluctuations in pressure [1]. The collapses can cause shock waves on the material surface, inducing erosive damage that can even dislodge particles [2]. These defects are potentially detrimental to the mechanical properties of the material, which provides an incentive to characterize and identify the defects composition as well as the process in which they are formed. This is explored in this thesis work.

## 1.2 Aim and Objectives

This study aims to identify and characterize surface defects in machined aluminium induced by ultrasonic cleaning. More specifically to understand the interaction between ultrasonic cleaning and the used detergent of 12 %*[volume]* *Formula 815 GD-NF* by inducing defects at different intensities and periods of time in in 2050 and 7050 aluminum. This aims to provide the answers to:

- Is there a difference in composition between the visible defects and the surrounding material?
- Are the visible defects results of adding or removing material from the surface?
- Is there a correlation between the two components of the defects: the surface colouration referred to as "clouds", and the pits?

- Is there a reason for the location of the defects?

### **1.3 Limitations**

The project was completed during 20 weeks at the beginning of 2020.

## 2 Theory

To be able to identify the type of damage or alteration of the aluminium surface and bulk it is important to understand the process and effect of ultrasonic cleaning on the cleaned parts, as well as the analysis tools used to obtain the information.

### 2.1 Ultrasonic Cavitation

When ultrasound, a mechanical wave with frequencies above the range of human hearing (i.e. greater than 20 kHz) to several MHz [3], passes through a liquid medium, it causes both the mechanical vibration of the liquid, as well as the physical movement of larger volumes. The interference of the ultrasound in the liquid will cause pressure drops in dissolved gas nuclei, appearing normally in most liquids at normal conditions, as well as shear the liquid, creating nucleation sites for bubbles. These drops create localized areas of pressure lower than the vapour pressure, causing bubbles to expand and grow until they grow to a size where they collapse violently from the outside pressure, as seen in Figure 1. The process of the growth and collapse of these micro-bubbles from ultrasonic interaction is what is known as *acoustic cavitation*. The physical process of cavitation is much the same as boiling, but instead of heating the liquid to its vapour transition temperature, the pressure is instead lowered, causing the vapour transition temperature to be lowered.

These near adiabatic bubble-collapses at high pressure of up to several thousand atmospheres, and temperatures of thousands of kelvins (up to 70 kbar and 14 kK according to W. Lauterborn *et.al.* [4]) generating micro-climates of extreme pressure and heat, as well as shockwaves, micro jets, shear forces and turbulence [5]. This will, in turn, generate reactive radicals. As an example,  $\bullet OH$  radicals will be generated by homolysis of water.

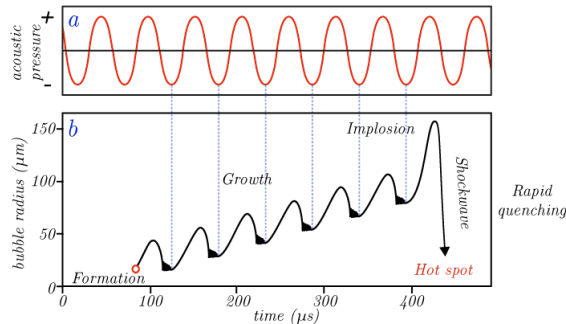


**Figure 1:** Graphical representation of the growth and collapse of acoustic cavitation bubbles. **a:** As the ultrasound interacts with the liquid, it experiences periodic compressions and decompressions. **b:** the bubbles formed by these phenomena oscillate until they reach a point of resonance and implode.

These extreme micro-climates are useful in several high-energy chemistry processes and have resulted in its own field of study; sonochemistry[6].

As the bubbles collapse they can collapse in two different manors, a *spherical*-, or a *non-spherical collapse*.

### 2.1.1 Spherical bubble collapse

As a bubble is subjected to an external pressure that is higher than its internal pressure, it is going to collapse rapidly, and if this happens at a certain distance from a surface, it will retain its spherical shape [7]. As the bubble collapses, surrounding water is drawn in towards the bubble centre at high speed, and as the water crashes into itself it emits a powerful *shockwave* that moves radially from the nucleus of the now gone bubble.

### 2.1.2 Non-spherical bubble collapse

As opposed to the spherical collapse, if a bubble collapses close to a rigid wall, it is generally assumed that it does not remain spherical if the distance from a wall is lower than 3 times their radius [7]. This non-spherical bubble will collapse in on itself towards the surface due to the surface tension of the bubble. This causes the bubble to collapse in on itself, shooting an in-compressible mixture of liquid and gas down towards the wall at speeds of  $\sim 600$  m/s as seen in Figure 2 [8]. As the jet impacts the surface, the bubble turns into a toroid shape before completely collapsing into smaller bubbles which may act as nuclei for the next generation of further bubbles. [9]

Further investigation into the micro-jet phenomenon show that only bubbles imploding in direct contact with the surface generate the most aggressive micro-jets at the highest speeds. This being due to the immense dampening effect of the liquid interface. Drastically reducing the depth and amounts of pitting caused by bubbles not in contact with the surface [10].

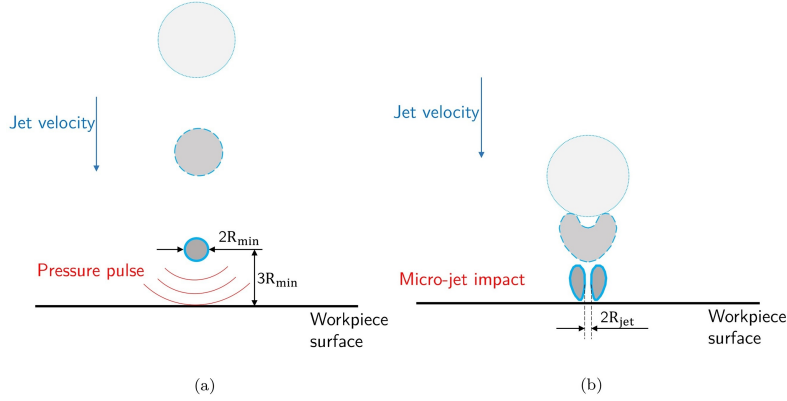


**Figure 2:** Illustration of the mechanical loading on the surface from the collapse of one cavitation bubble in two different types of collapse. **a** a spherical bubble collapse more than three times the radius away from the surface and its resulting pressure pulse emission. **b** a non-spherical bubble collapse less than three times the radius away from the surface and its resulting pressure micro-jet formation and impact.

### 2.1.3 Geometric influence

As cavitation behaviour is dependent on the surroundings of the cavitating bubble, geometry of the sample plays a big role on the quantity of bubble impacts on a surface. As surface area increases, so does the probability of a bubble forming close enough to form a micro jet, indicating that a rougher surface will erode faster. It

will also have larger numbers of nucleation sites, further increasing the probability of new bubbles forming.

Jean-Pierre Franc *et.al.* showed in a study that velocity of the surrounding fluid played a role on both size, and quantity of pitting associated with cavitation. As the velocity of the liquid increased, the size of the pits increased, at the same time as the amounts of pits increased [11].

## 2.2 Ultrasonic cleaning

Ultrasonic cleaning is a technique with a definite place in a wide variety of use-cases, where of course the use in heavy industry has been a prevalent field from it's earliest of days in the 1950:s where it was first implemented[12]. The energy released from an implosion close to the surface collides, disturbs and agitate the contaminants allowing detergents and cleaning solution to penetrate the layer and hence increase the cleaning speed and efficiency. The dynamic pressure waves aid in the cleaning process by aiding with transporting the fragmented contaminants away. The force created also provide the mechanical energy to break apart the contaminants. Perhaps the biggest advantage over conventional mechanical agitation is that due to the object being submerged and covered by evenly distributed ultrasonic waves full, or close to full effect can reach and penetrate crevices, blind holes, and areas otherwise inaccessible by traditional means. Leading to a uniform and consistent result, regardless of geometry and complexity of the parts.

### 2.2.1 Cavitation erosion

Cavitation erosion is the complex phenomenon where a gradual degradation of a solid surface is caused by interaction with imploding cavitation bubbles. That is why it is generally considered that the intensity of the cavitation load is directly related to the mass loss of the exposed material. The cavitation load is the combined load of the impacts from the generated cavitation bubbles and micro-jets that impact the surface.

Attempts to measurements of the impact of a single cavitation bubble, as well as from groups of bubbles has been performed for years since Knapp [13] in 1955 first described the phenomenon. He also discovered that only a few of all the cavitation bubbles were able to cause pitting damage, and that these amounts increased logarithmically with the velocity of the flow. In 1966 Benjamin and Ellis documented the asymmetrical deformation of vapour bubbles when in the vicinity of a solid boundary layer, which caused the water around the collapsing cavitaional bubble to form a micro-jet piercing the bubble [14].

The effect of the cavitation erosion on the surface will in many cases be visible taking on different shapes and sometimes colours as it can result in both changing the surface texture and composition by either erosion, oxidation, or corrosion [15]. These types of effects will in this thesis be referred to as "*clouds*".

## 3 Experimental

### 3.1 Materials

The samples were made from two alloys, AA7050-T7451, and AA2050-T84. Which will be referred to as simply "7050" and "2050" from here on. two important alloys for the aerospace industry due to their high strength and light weight. 7050 is an alloy where the main alloying elements are Zn, Cu, and Mg. Whereas Cu and Li are the main elements apart from aluminium in 2050. Nominal compositions can be seen in Tables 1 and 2. These alloys had been cast into slabs, from which the samples were produces as seen in Figure 3.

**Table 1:** Chemical composition of the 2050 Al-alloy.

Chemical composition [vol.%]													
	Cu	Li	Ag	Mg	Mn	Zn	Zr	Fe	Ti	Si	Cr	Other	Al
<b>Min</b>	3.2	0.7	0.2	0.2	0.2	-	0.06	-	-	-	-	-	Rest
<b>Max</b>	3.9	1.3	0.7	0.6	0.5	0.25	0.14	0.1	0.1	0.08	0.05	0.15	Rem

**Table 2:** Chemical composition of the 7050 Al-alloy.

Chemical composition [vol.%]											
	Zn	Cu	Mg	Zr	Fe	Si	Mn	Ti	Cr	Other	Al
<b>Min</b>	5.7	2.0	1.9	0.08	-	-	-	-	-	-	Rest
<b>Max</b>	6.7	2.6	2.6	0.15	0.15	0.12	0.1	0.06	0.04	0.15	Rem

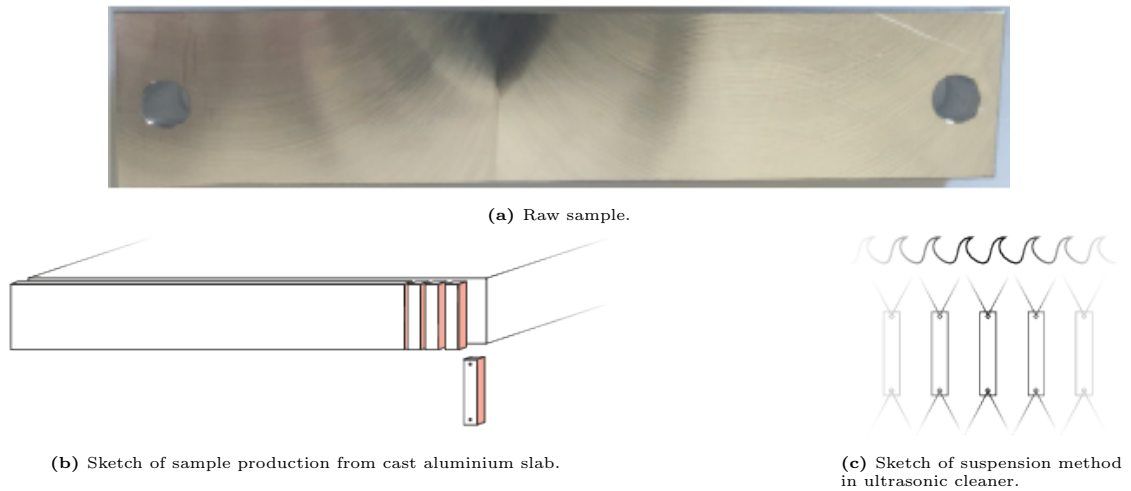


**Figure 3:** Images of the sample production process.

The Samples were face milled in preparation of the tests aiming for a surface roughness of  $R_a \approx 0.8 \mu m$

### 3.2 The effect of the cleaning solution on the surface

Two samples were left in a 12 % [volume] cleaning solution, produced by Bio-Clean, called *Formula 815 GD-NF*. This Cleaning solution is a non-corrosive solution to alloys and most non-ferrous metals. The samples were placed without any agitation for 0, 30 and 60 minutes.

### 3.3 Samples ultrasonically cleaned at different intensities

The test procedure was based on suspending several sample pieces in an ultrasonic bath as sketched in Figure 3c. The samples were then allowed to go through an increasing numbers of cleaning cycles, each 6 minutes long. The first batch of two samples was run at 100 % intensity for 2 cycles. This intensity is enough to induce big and visible defects on the surface. The following 7 samples were run at 50 % intensity, and samples were taken out after 2, 4, 6, 8, 10, and 18 cycles. These were produced to reveal how the surface roughness develop over time, as the lower intensity results allows for a better insight.

### 3.4 Surface roughness evaluation and presentation

The samples were studied in VSI(vertical scanning interferometry) where random areas were selected at roughly the same distance from the side of the material to avoid roughness in-variance due to coring. and its potential effect on roughness development. The software ZYGO Mx Software was used to create images of the surfaces, and  $R_a$  data from five different sites per sample for the general surface measurements were acquired using 20x magnification in the Veeco Vision software, and standard deviation calculated for these. For the pit and cloud measurements values were acquired using the ZYGO Mx Software directly.

### 3.5 Pre- and post characterization of the surfaces

The surface roughness and material transfer was studied in a FEG-SEM, using low acceleration voltage to allow for surface sensitivity. The sample was also tilted 60° to allow for better topography imaging. EDS analysis was used to acquire information regarding the elements, this was acquired at 20 kV to allow for some information deeper in the material as the pitting indicated that particles were most likely of a size big enough that they would not only be found on the surface.



## 4 Results

### 4.1 Surface appearance and elemental analysis

#### 4.1.1 General observations on the similarities between 2050 & 7050

Typically, the two alloys behaved the same, showing the same general tendencies in almost every test. That is why most results are only reported for one of the alloys.

LOM(light optical microscope) imaging of the surface shows clear traces of the milling lines from the production. Most surfaces are also covered in scratches in other angles compared to the milling marks. These are the result of rough handling and are a product of how the samples have been scratched in transport. These scratches also seem to contain darker patches of material, something EDS analysis confirms to be a higher concentration of carbon, meaning that it is most likely surface contaminants becoming trapped in the rougher surface texture.

#### 4.1.2 Surface appearance of the raw samples

Examination of the raw surface using imaging in SEM(scanning electron microscope) using BSE(backscattered electrons) show particles and areas separating from the aluminium matrix, see Figure 4. These areas are rich in different elements Cu, Mg, Fe, Si and Mn varying from site to site, see Figure 5.

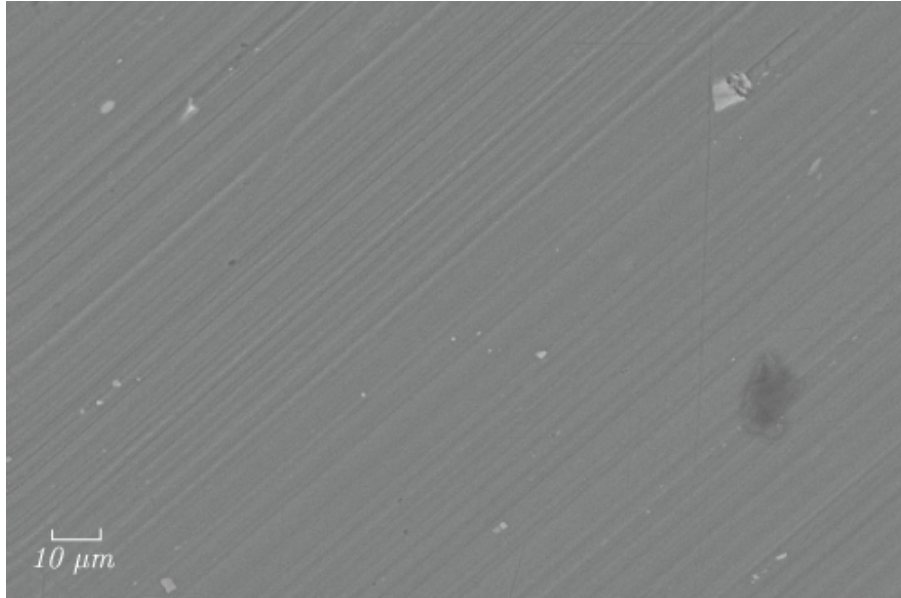
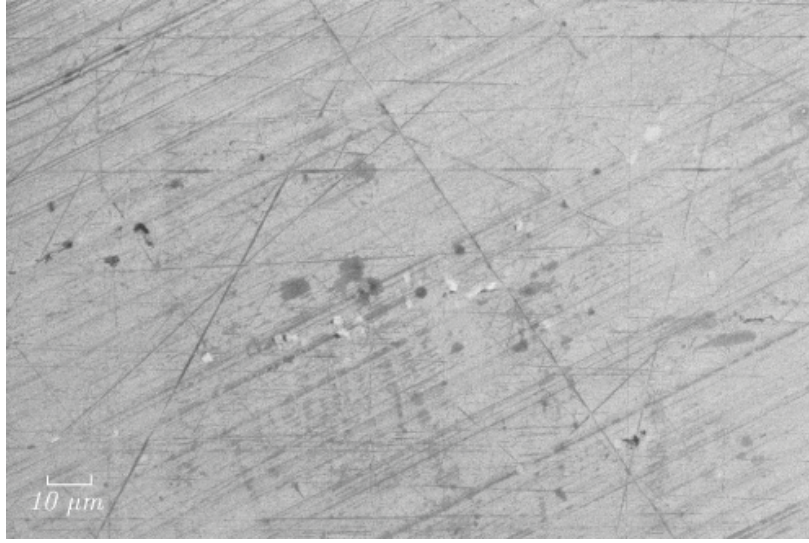
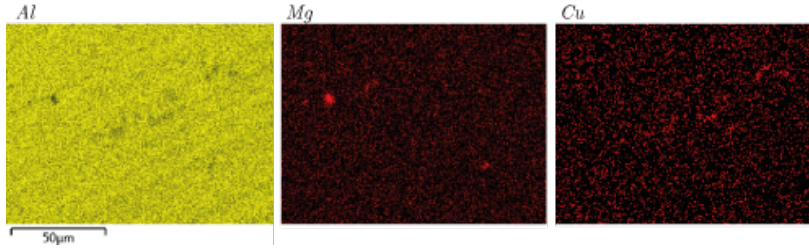


**Figure 4:** BSE image of 7050 surface on a raw sample, showing lighter particles that show up as Cu and Fe rich areas.



(a) Surface showing lighter areas identified as separated elements from the alloy, as well as darker areas most likely carbon contaminants.



(b) EDS spectrum.

**Figure 5:** Representative of the average surface of a raw 7050-sample. SEM-image. The separated elements have been identified using the EDS maps in the bottom row (Al, Mg, Cu; 20 kV).

#### 4.1.3 Samples ultrasonically cleaned at 50 % intensity

The surface roughness measurements on the 7050 alloy from the 50 % intensity ultrasonic cleaning show that the initial value is relatively low ( $R_a = 0.56\mu m$ ) and fluctuates around this value until it suddenly shows a steep increase after 60 minutes see Figure 6. During the cleaning cycles, the surface takes on a more spotty appearance, at the same time as the number of pits increase, as can be seen in Figures 7a and 7b. Figure 7c refers to samples left in the cleaning solution without any ultrasonic effect, and will be discussed in a later section.

#### 4.1.4 Samples ultrasonically cleaned at 100 % intensity

The samples cleaned at 100 % intensity showed tendencies to big pits,  $\sim 10$  times bigger than the pits in the samples cleaned at 50 % intensity, see Figures 8 and 9. These pits were almost always accompanied by a big cloud on the surface. However, no clouds were found without an associated pit. These clouds were almost exclusively in the shape of a comet trail, but there were also instances of round shapes. There was no common directionality of the clouds, instead, they seemed to be pointing in random directions.

Closer inspection in SEM confirmed that the clouds are an increase in surface rough-

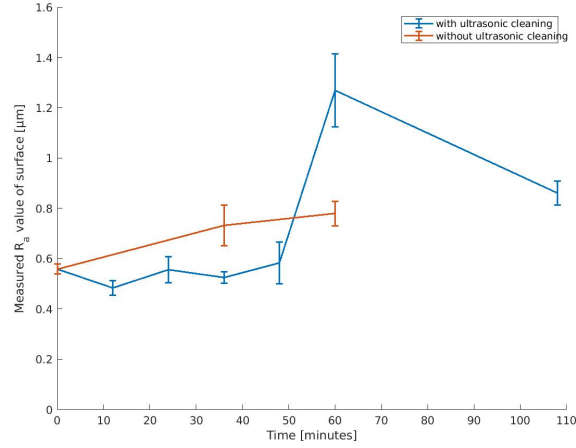


**Figure 6:** Average of five measurements. Values with standard deviation of  $R_a$  values against time. The blue graph shows results from samples cleaned with an ultrasonic cleaner turned on at 50% intensity. The red line shows samples left in the cleaning solution with the ultrasonic cleaner turned off.

ness, see Figure 10. Performing an element analysis using EDS on select areas around the pits and clouds confirmed that there was no change in material composition in the affected area, compared to an area without the increase in roughness. There were also areas around the pits, as well as on the rim of the pits where the composition indicated that a separation had occurred, see Tables 3 and 4 for quantitative analysis for each of the alloys.

A better look at the surface roughness and topography of the pit and its surroundings are achieved by tilting the sample to 60°. This shows a smooth inside of the pits, as well as fatigue lines. The surrounding topology seems to indicate that a bigger area was deformed as the surface shows signs of being shifted around the pits, as seen in Figure 10

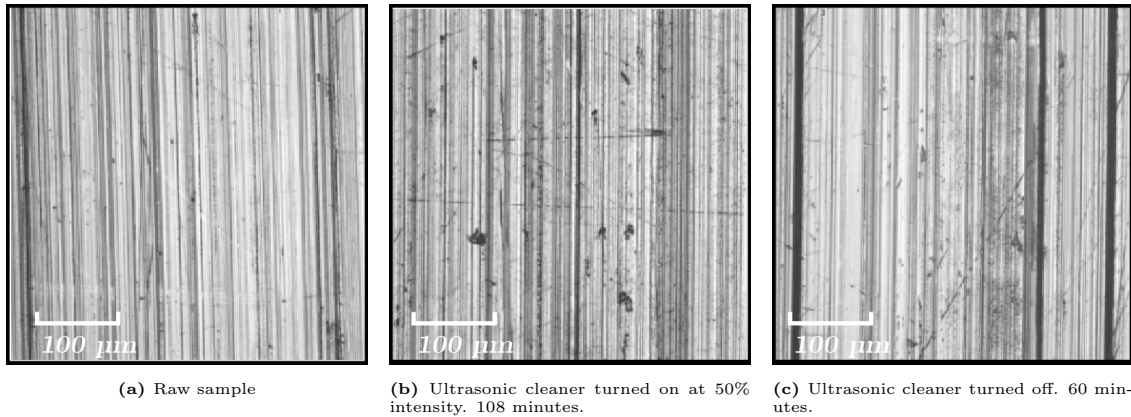


**Figure 7:** Typical LOM image of representative 7050 surface.



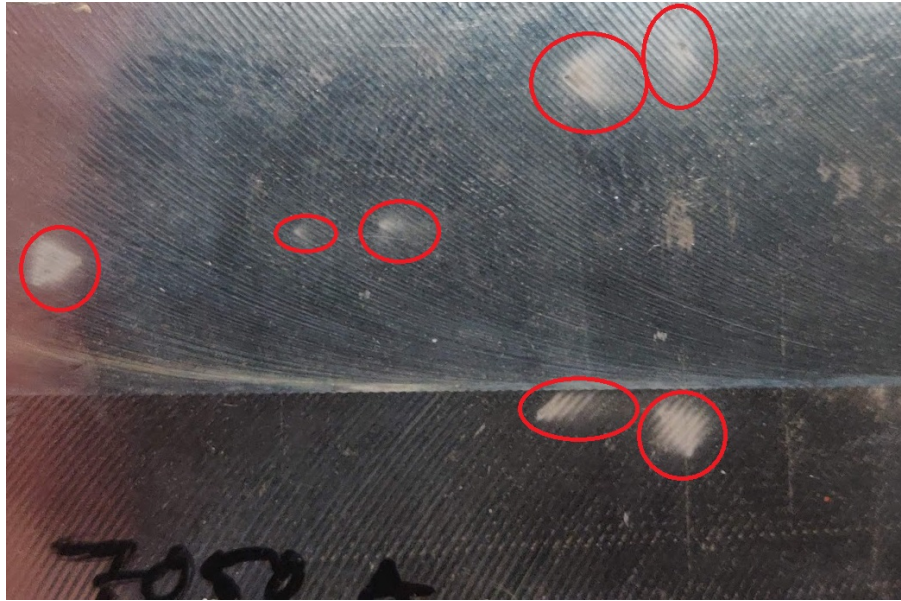


**Figure 8:** LOM image of a sample, pits and clouds marked with red rings.

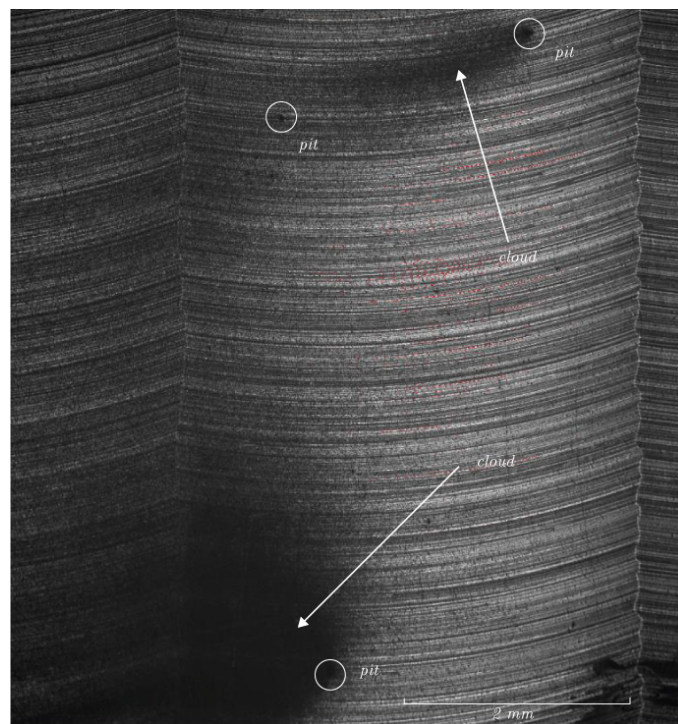
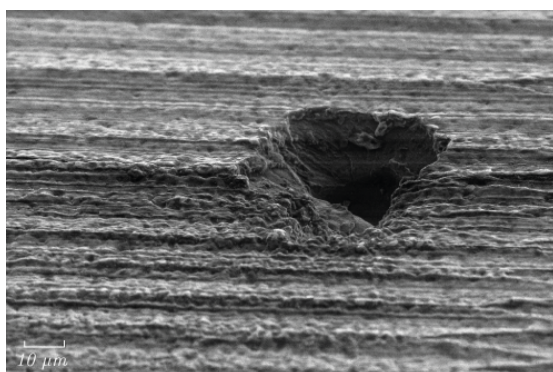
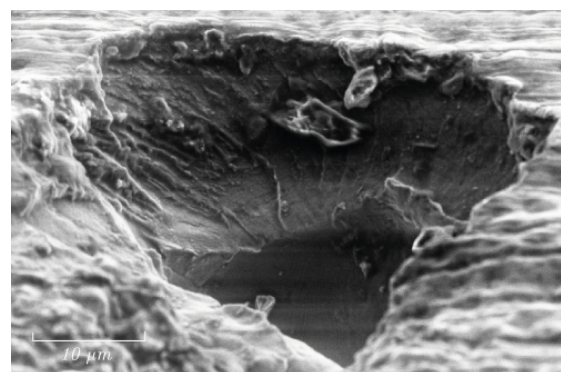


**Figure 9:** Representative LOM image of area with pits and clouds, bigger ones marked in image.



**(a)** Surroundings show deflected material towards the pit.



**(b)** Higher magnification of the pit, showing fatigue lines and a smooth surface texture.

**Figure 13:** Pit tilted at 60° for better contrast at two magnifications.

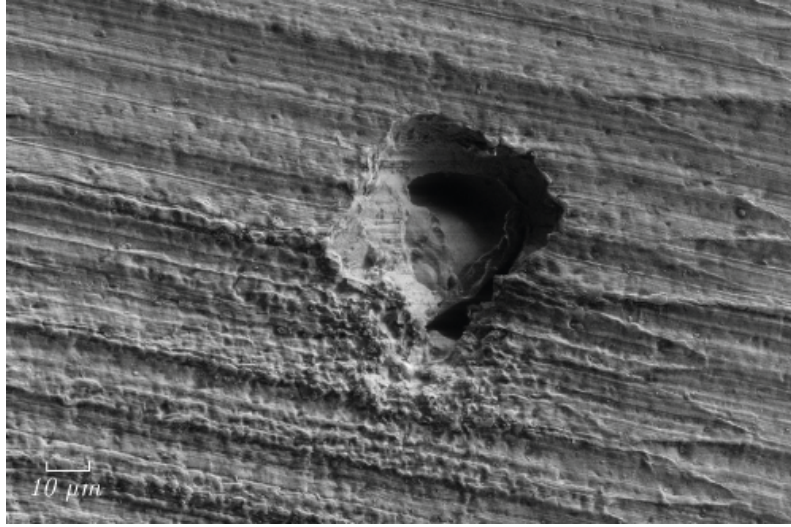


**Figure 10:** Image of typical pit. Cloud direction is downward in the image. SEM secondary electron image.

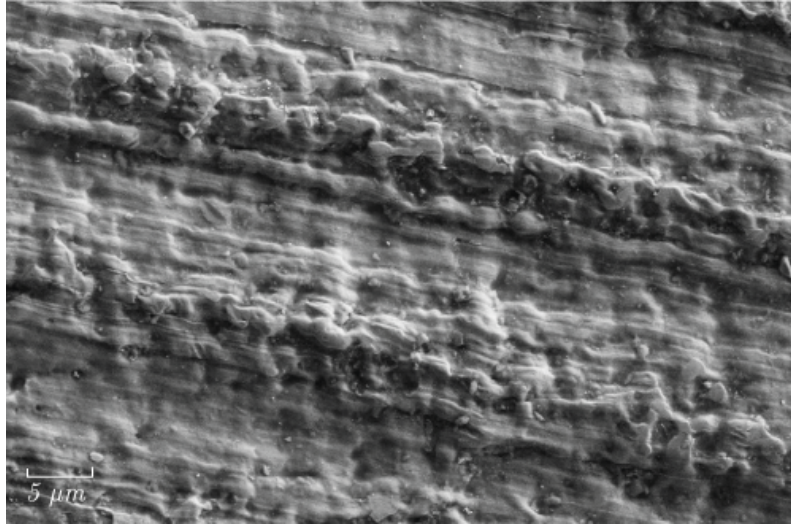
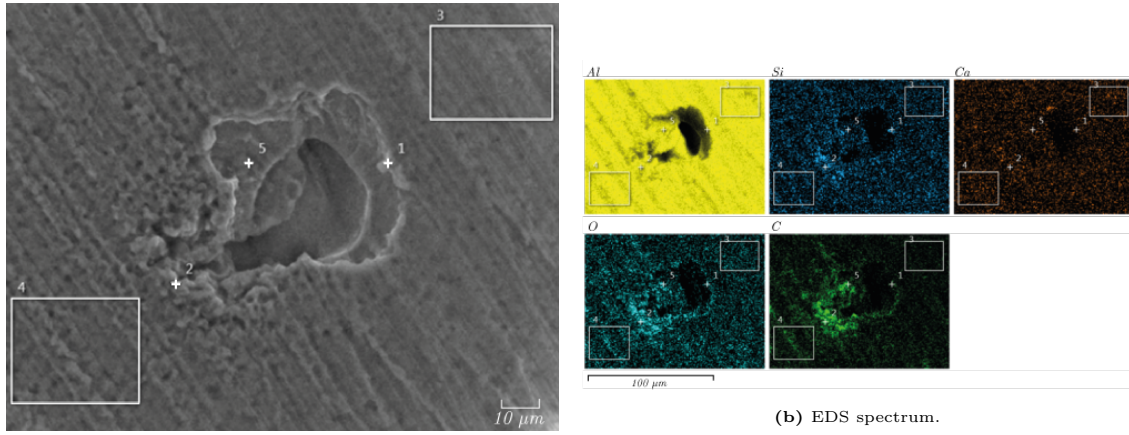


**Figure 11:** Magnified image of a cloud. SEM secondary electron image.

#### 4.1.5 Influence of cleaning process duration on general surface roughness

The surface roughness on the samples left in the cleaning liquid without any ultrasonic effect also show an increase, but a smaller, and more linear one, compared to samples being ultrasonically cleaned, see Figure 6. The surface appearance also became rougher in the same way as the one that had been exposed to ultrasonic cleaning, but with far fewer large pits as can be seen when comparing Figures 7b and 7c.





(a) Same hole as in fig. 10 but rotated 45 °. Element quantification spots are marked.

**Figure 12:** SEM image where areas for further element identification are marked. The separated elements have been identified using the EDS maps in the bottom row (Al, Si, Ca, O, C; 20 kV).

**Table 3:** Quantitative EDS analysis of 2050 sample after 12 minutes of ultrasonic cleaning at 100 % intensity.

7050 elements	Location			
	Surface defect "cloud" (%At)	Unaffected surface (%At)	Pit edge (%At)	Inside of pit (%At)
C	21.1	10.1	66,5	21.7
N	0	0.8	0	15.4
O	2.4	1.4	7.7	12.2
Na	0	0	0	0.3
Mg	0.2	0	0	0.3
Al	63.6	63	24.8	61.1
Si	0.3	0	0.4	0.2
S	0	0	0	0.2
Cl	0	0	0	0.7
K	0	0	0	0.1
Ca	0	0	0	0.1
Mn	0.3	0.3	0	0.1
Fe	0	0	0	0
Cu	2.4	2.8	0.7	1.9
Zn	0	0	0	0.3
Ag	0.2	0.4	0	0.3

**Table 4:** Quantitative EDS analysis of 7050 sample after 12 minutes of ultrasonic cleaning at 100 % intensity.

7050 elements	Location			
	Surface defect "cloud" (%At)	Unaffected surface (%At)	Pit edge (%At)	Inside of pit (%At)
C	11.3	8.8	5.8	63.8
O	2	1	1	18.8
Na	0.6	0.6	0	2.7
Mg	1.7	1.8	0.9	0.3
Al	76.6	79.9	58.8	8
Si	0.2	0.1	0	0.3
S	0	0	0	0.1
Cl	0	0	0	2.6
K	0	0	0	1.8
Ca	0.1	0	0	0.4
Fe	0	0	0.7	0.2
Cu	2	2.1	9.4	0.3
Zn	5.6	5.8	23.5	0.7

## 5 Discussion

### 5.1 Surface overview and imaging

The results demonstrate that the relationship between the roughness, pits and clouds have a clear dependency on ultrasonic settings, as well as precipitated elements from the alloy. However, the results are not conclusive to why the pits appear where they do, nor why they appear in the shape of a large pit from a single event, rather than multiple minor events interacting.

#### 5.1.1 Effects of the cleaning liquid and ultrasonic washing on material surface

As the  $R_a$  measurements show, the roughness increase over time, both when having the sample submerged in the cleaning fluid with the ultrasound turned off, but also for the sample where the ultrasonic cleaner was turned on. In the case of the samples in the cleaning solution without any ultrasonic cleaning, it seems likely that this is due to an etching effect on the surface. The formula is specially designed to be used with alloys and non-ferrous metals. It is mentioned to be able to clean ferrous metals in the case of carbon- and stainless steels on the company website, however as EDS analysis shows, there are plenty of areas where elements have precipitated from the alloy, and in some cases sit on the surface of the sample. The ferrous areas of these might very well be subjected to an etching effect, causing the surface roughness to increase, as well as create weaker areas and points of attack for micro-jet phenomena. Considering that the samples go through a very rough milling process before being measured upon, it might also be the case that the cleaning solution simply has worked and started removing surface contaminants from the surface, and in doing that also increasing the surface roughness. This would however eventually prove to cause the increase in roughness to eventually decrease and stop as all removable contaminant is removed. As this test only went on for 60 minutes it is hard to draw any hard conclusions whether what we are seeing is a result of either of those theories from this test alone.

The roughness behaviour of the sample being ultrasonically washed at 50 % intensity seen in fig. 6 show that at first no change is seen. But after 40 minutes a sudden jump is followed by a slightly higher value than baseline. Most likely this is due to the ultrasonic intensity being low enough that the cavitation is not strong enough to cause immediate erosion of the surface. But as earlier mentioned, the erosion follows a logarithmic growth as the surface area increases with roughness, leading to an increase in erosion speed. This would indicate that as erosion starts, it will show a steep increase in roughness development. The graphs strange behaviour in our case is most likely due to inconsistency in the original roughness value of the surface where measurements were taken due to its surface topology from how it was milled.

### 5.1.2 Pit and cloud development and characterization

As only smaller pits ( $< 3\mu m$ ) were formed on the surface of the sample washed in 50 % intensity, even after 108 minutes, it is safe to assume that some sort of threshold is crossed when increasing the efficiency of the ultrasonic cleaner to 100 % intensity. The pattern of large pits appearing without an accompanying cloud, but not vice versa seems to confirm that the clouds are a product of the holes, and not the other way around. This is further exemplified as the inside surfaces of the pits are smooth and show fatigue lines, rather than the rough surface we would expect with the exponential growth of material removal from smaller bubble collapse. S.Shrestha *et.al.* show that cavitation erosion on mild steel can dislodge larger particles when they have been dissolutioned from the matrix as hard-phase particles on the surface[16]. Therefore it seems likely that it indicates a large impact from a micro-jet phenomenon which has excavated a larger particle, perhaps weakened by the etching of a separated ferrous precipitate.

H. Chen [17] further showed on mild steel that the clouds, or "rings" as they refer to the phenomenon, was the result of oxidation from increased temperatures. This indicates that the phenomena is the result of cavitation erosion rather than of a corroding agent emanating from a growing pit. And that the different shapes of the rings are attributed to the different bubble shapes at the moment of collapse. also stemming from the effect of the relative distance and speed of the bubble to the metal surface.

Therefore it seems highly likely that the heated jet of the micro jet would then cause the surface to go through a transformation forming harder oxides, which would then be broken up and removed by smaller shockwave phenomena, accelerating the erosion process vastly in the area affected by the micro jet impact. This would also explain the directionality, as the micro jet impacting on an angle would create a heated zone in much the same shape of the comet trails that are seen. This theory becomes more believable as the EDS analysis show that there is an increase in alloying elements on the side, and sometimes inside of the pits. This is made more probable due to that the parts were prepared with a milling action. This relatively harsh surface profiling method will have broken up the surface grains and destroyed many of the potential surface phases which could have acted as points of attack if more brittle or susceptible to etching from the cleaning liquid, thus making it so that these phenomena only occur in fewer spots rather than more often across the whole sample surface.



## 6 Conclusions

The effect of ultrasonic cleaning and one washing fluid on two aluminium alloys have been investigated in a small scale test in this thesis. The tests included:

- leaving a sample in cleaning fluid, to see its effect on the surface roughness.
- cleaning samples at 50 % intensity at an increasing length of time to investigate the effect of ultrasonic cleaning over time on the surface roughness.
- cleaning samples at 100 % intensity and analyze the pits and clouds that form to characterize them.

The surface roughness was found to increase both with time in the cleaning solution, as well as when ultrasonically cleaned

- Surface roughness increased linearly when left in the cleaning solution
- Surface roughness was stable up until 40 minutes
- The cleaning fluid is likely etching the precipitate making it susceptible to be flaked off, or act as points of attack for other material removals when hit by a micro jet bubble.

When cleaned at 100 % intensity, surface defects in the shape of pits and clouds were created. These allows us to answer our original questions.

- *Is there a difference in composition between the visible defects and the surrounding material?*
  - there are signs of precipitate elements near, or in the pit of the defect. The cloud part is however too thin to accurately measure using the methods used in this setup.
- *Are the visible defects results of adding or removing material from the surface?*
  - As micro jet impact is the most likely source of the larger pit and clouds. The pit is probably formed by removing a big piece of material, and the cloud is formed by the formation of more brittle material like oxides on the surface where the heat from the micro jet impacts. This more brittle surface is then broken up by the following shock waves from spherical bubble collapses.
- *Is there a correlation between the two components of the defects: the surface colouration referred to as "clouds", and the pits?*
  - The pits and clouds are connected in such that a cloud is always found connected to a pit.
- *Is there a reason for the location of the defects?*
  - Segregates cause a change in composition moving toward the centre of the sample explaining the defect being prone to appear close to the middle part of the sample.

- Cavitation is more likely to be a problem where standing bubbles can form, such as on rougher surfaces, and in areas of complex geometry

Interestingly, both alloys showed almost identical results through all tests, only differing in what elements seems to precipitate due to the elements in the alloy.

*In short* most of the questions this thesis set out to answer have been answered, there is still however a lot of room for further development. The results tell us that the ultrasonic part, as well as the solution itself both increase surface roughness of the samples. When crossing a threshold in ultrasonic intensity micro jet cavitation can dislodge precipitates, or areas weakened by precipitate to form a large pit. And the following heat from the jet causes the surface to oxidise, becoming more brittle, and be broken up by other cavitation phenomena to cause rapid acceleration of surface roughness in an area originating from the pit.

## 7 Further research

Lapping the sample surface to a much smoother surface finish would give much better results when comparing roughness development in all cases.

Performing a surface-sensitive analysis to see whether the oxide on the surface in the clouds has a different composition from the surrounding area.

Selecting areas on the surface of the raw sample, and analyzing them in between shorter wash cycles at 100 % intensity to better capture the development of the pits and clouds, as well as to identify common denominators of the surface where the pits are formed.

## References

- [1] J. R. Davis. *Corrosion of aluminum and aluminum alloys*. ASM International, Materials Park, OH, 1st edition, 1999.
- [2] Brijesh Vyas and Carolyn M. Preece. Cavitation erosion of face centered cubic metals. *Metallurgical Transactions A*, 8(6):915–923, 1977.
- [3] David J. Martin, Irving T. P. Wells, and Christopher R. Goodwin. Physics of ultrasound. *Anaesthesia and Intensive Care Medicine*, 16(3):132–135, 2015.
- [4] W. Lauterborn, T. Kurz, R. Geisler, D. Schanz, and O. Lindau. Acoustic cavitation, bubble dynamics and sonoluminescence. *Ultrasonics - Sonochemistry*, 14(4):484–491, 2007.
- [5] Muthupandian Ashokkumar. The characterization of acoustic cavitation bubbles – an overview. *Ultrasonics - Sonochemistry*, 18(4):864–872, 2011.
- [6] Juan C. Colmenares, Gregory Chatel, and SpringerLink (Online service). *Sonochemistry: From Basic Principles to Innovative Applications*. Springer International Publishing, Cham, 1st 2017 edition, 2017.
- [7] Emmanuel Sonde, Thibaut Chaise, Nicolas Boisson, and Daniel Nelias. Modeling of cavitation peening: Jet, bubble growth and collapse, micro-jet and residual stresses. *Journal of Materials Processing Tech*, 262:479–491, 2018.
- [8] W. Lauterborn and H. Bolle. Experimental investigations of cavitation-bubble collapse in the neighbourhood of a solid boundary. *Journal of Fluid Mechanics*, 72(2):391–399, 1975.
- [9] Y Tomita and A Shima. Mechanisms of impulsive pressure generation and damage pit formation by bubble collapse. *Journal of Fluid Mechanics*, 169:535–564, 1986.
- [10] A Philipp and W Lauterborn. Cavitation erosion by single laser-produced bubbles. *Journal of Fluid Mechanics*, 361:75–116, 1998.
- [11] Jean-Pierre Franc, Michel Riondet, Ayat Karimi, and Georges L. Chahine. Material and velocity effects on cavitation erosion pitting. *Wear*, 274-275:248–259, 2012.
- [12] Mason Timothy J. Ultrasonic cleaning: An historical perspective. *Ultrasonics - Sonochemistry*, 29:519–523, 2016.
- [13] Robert Knapp. Investigation of the mechanics of cavitation and cavitation damage. *Transactions of the ASME*, 06 1957.
- [14] T. B. Benjamin and A. T. Ellis. The collapse of cavitation bubbles and the pressures thereby produced against solid boundaries. *Philosophical Transactions of the Royal Society of London. Series A, Mathematical and Physical Sciences*, 260(1110):221–240, 1966.

- [15] Jiang Li, Bo Wu, and Haosheng Chen. Formation and development of iridescent rings around cavitation erosion pits. *Tribology Letters*, 52(3):495–500, 2013.
- [16] S. Shrestha, T. Hodgkiess, and A. Neville. Erosion–corrosion behaviour of high-velocity oxy-fuel ni–cr–mo–si–b coatings under high-velocity seawater jet impingement. *Wear*, 259(1):208–218, 2005.
- [17] Haosheng Chen. Iridescent rings around cavitation erosion pits on surface of mild carbon steel. *Wear*, 269(7):602–606, 2010.